

Prof. Wei Yi
Associate Editor
IEEE Transactions on Signal Processing

January 3, 2025

Response to Decision on Manuscript T-SP-32387-2024

Dear Editor and Reviewers,

Thank you for giving us the opportunity to submit a revised version of *Channel Shaping Using Beyond Diagonal RIS: Analysis, Optimization, and Enhanced Flexibility*. Your comments and suggestions have been invaluable in helping us improve the quality of the manuscript. Below we prepare a point-to-point response and highlight the corresponding in-text changes, where labels have been matched to the latest version for your convenience. The title has been changed to *MIMO Channel Shaping and Rate Maximization Using Beyond Diagonal RIS* to better reflect the content of the manuscript. We hope that the revisions and clarifications make the manuscript meet the standards of TSP publications.

Yours sincerely,

Yang Zhao, Hongyu Li, Bruno Clerckx, and Massimo Franceschetti

Editorial Decision

The reviewers raised a number of concerns regarding the paper's contribution, novelty, and mathematical correctness, which led to the recommendation for rejection. The main issues identified include:

- (a) The contribution of the paper is unclear. Specifically, the proposed framework in (25) is not sufficiently general as it does not consider Beyond Diagonal (BD)-Reconfigurable Intelligent Surface (RIS) dependent constraints (e.g., Quality of Service (QoS), sensing quality). A more general case has already been investigated and solved in the authors' previous work [41]. Some content in Section III-B are well established methods in the literature [58].
- (b) The optimization problems (39) and (36) lacks of novelty. The reviewer pointed that they can be possibly solved by existing methods through appropriate adjustment [33, 57]. Also, it is also pointed out that Corollaries 3.1 – 3.2 are the standard results from matrix textbook.
- (c) The correctness and usefulness of the mathematical derivations. For example, the derivation in the proof of Appendix H is incorrect. Convergence proof in Appendix J is questionable. The usefulness of these bounds on singular values of the effective channel \mathbf{H} is unclear.
- (d) The literature review can be enhanced to cover a boarder range of papers that related to the problem addressed.
- (e) The simulation study can be enhanced. For example, comparisons with the Diagonal (D)-RIS and a globally passive BD-RIS were suggested by the reviewer.

Response We appreciate the editor's summary of the comments. We have carefully considered each point raised and have made significant revisions to address these concerns. Please refer to the following responses for a detailed explanation of the changes made in the revised manuscript.

Reviewer 1

This manuscript investigates the impact of BD-RIS to the distribution of singular values of Multiple-Input Multiple-Output (MIMO) channel of a point-to-point communication system. Especially, the authors derive bounds of singular values of BD-RIS channel and propose algorithms to design BD-RIS configuration.

1.1 *The contribution of Sec. III-B is unclear for the following two reasons.*

- (a) *The manuscript claims to propose a universal optimization framework for BD-RIS as in (25). However, the framework in (25) is indeed not sufficiently general. It does not consider BD-RIS dependent constraints (e.g., QoS, sensing quality) besides the orthogonal conditions (25b). The reviewer notice that a more general framework, which considers BD-RIS constraints in addition to (25b), has already been investigated and solved in the authors' previous work [41].*
- (b) *Besides, both the non-geodesic Riemannian Conjugate Gradient (RCG) and geodesic RCG algorithms, e.g., (27) – (33), are well established methods in the literature, e.g., [58]. Therefore, the novelty of Sec. III-B unclear.*

Response We appreciate the reviewer's insightful comments. The claim of “universal optimization framework” and the non-geodesic RCG method have been removed from the revised manuscript, and we have carefully rephrased Sections I-C and III-B to reflect the specific contributions of our work. Indeed, the geodesic RCG algorithm is well studied in the literature and our intention was to extend it to block-unitary cases with parallel or unified updates, which is particularly suitable for the design of group-connected BD-RIS.

1.2 In Sec. III-B, the manuscript proposes to maximize weighted sum of singular values of the effective channel \mathbf{H} . The optimization objective is rather vague. Is the weighted sum of singular values related to any meaningful performance metric (e.g., capacity, power gain, and so on)?

Response We agree with the reviewer that the optimization objective of weighted sum of singular values is not directly related to a specific performance metric. However, it helps to reveal the achievable region of channel singular values (which covers all related metrics) and we believe itself could serve as a metric for measuring the MIMO channel shaping capability of different RIS. In the revised manuscript, we also generalize the objective to symmetric gauge functions to further address this concern.

Consider a special class of channel shaping problem

$$\begin{aligned} \max_{\boldsymbol{\Theta}} \quad & f(\text{sv}(\mathbf{H})) \\ \text{s.t.} \quad & \boldsymbol{\Theta}_g^H \boldsymbol{\Theta}_g = \mathbf{I}, \quad \forall g, \end{aligned}$$

where $f: \mathbb{R}^N \rightarrow \mathbb{R}$ is a symmetric gauge function (i.e., a norm invariant under sign change and argument permutation) [56]. Examples of such f include the Ky Fan k norm, Schatten p norm, n -th singular value, and channel power gain.

1.3 Derivation in the proof of Appendix H is incorrect. Specifically, $(\partial \mathbf{u}^T) \cdot \mathbf{u}$ is not equal to $\partial(\mathbf{u}^T \mathbf{u})$. Similar error occurs to \mathbf{v} . Please note that the derivative of singular value of a matrix with respect to the matrix itself does not exist. In fact, sub-differential should be used instead, e.g., [i].

Response We appreciate the reviewer's careful reading of the manuscript. We have corrected the derivation in the proof of Appendix H and have used the sub-differential to handle the non-differentiability of the singular value function.

Proposition 4. The sub-differential of (25a) with respect to BD-RIS block g is

$$\partial_{\boldsymbol{\Theta}_g} f(\text{sv}(\mathbf{H})) = \text{conv}\{\mathbf{H}_{B,g}^H \mathbf{U} \mathbf{D} \mathbf{V}^H \mathbf{H}_{F,g}^H\},$$

where $\mathbf{D} \in \mathbb{C}^{N_R \times N_T}$ is a rectangular diagonal matrix with $[\mathbf{D}]_{n,n} \in \partial_{\sigma_n(\mathbf{H})} f(\text{sv}(\mathbf{H}))$, $\forall n \in [N]$, and \mathbf{U}, \mathbf{V} are any left and right singular matrices of \mathbf{H} .

1.4 The rank equation in the proof of Prop. 1 (Appendix A) seems confusing. The rank of product of two matrices is: $\text{rank}(\mathbf{A}\mathbf{B}) = \text{rank}(\mathbf{B}) - \dim(\ker(\mathbf{A}) \cap \text{ran}(\mathbf{B}))$. How could one obtain the rank equation in Appendix A? Please clarify.

Response Using the rank equation pointed out by the reviewer, we realized that the achievability proof in the previous version was incorrect. In fact, the proposition was incorrect. A new proof in Appendix A shows that BD-RIS may achieve a larger or smaller number of MIMO Degrees of Freedom (DoF) than D-RIS. We apologize for the confusion and appreciate the reviewer for pointing out this mistake.

Proposition 1 (Degrees of freedom). BD-RIS may achieve a larger or smaller number of MIMO DoF than D-RIS.

1.5 In Sec. III-A, the manuscript provides a number of bounds on singular values of the effective channel \mathbf{H} . However, the usefulness of these bounds is unclear. What can these bounds be used for? Note the results in Corollaries 3.1 – 3.2 are quite standard results from matrix textbook. The (upper) bound in Corollary 3.4, which is achieved by aligning its left and right singular-value vectors to that of the forward and backward channels, respectively, is reminiscent of the results in seminal papers on relay beamforming design, e.g., [ii, iii].

Response The aim of Proposition 3 is to transform the channel shaping limit question into a well-studied linear algebra question, such that Corollaries 3.1 – 3.2 (previously 3.1 – 3.4) follows from standard results. In the revised manuscript, we have also added

- Upper and lower bounds on individual singular value in Corollary 3.3;
- Lower bound on channel power gain in Corollary 3.4;
- Upper bound on channel capacity at general and extreme Signal-to-Noise Ratio (SNR) in Corollaries 3.5 and 3.6;

and derived the corresponding RIS scattering matrices in closed form. We also notice that the bounds on the n -th singular value can be used, for example, to simplify the precoder design in MIMO systems with limited number n of RF chains. The comparison to relay beamforming design is insightful and we have added footnote 13 to highlight the connection.

Corollary 3.3 (Individual singular value). *If the direct channel is negligible, then the n -th channel singular value can be manipulated up to*

$$\max_{i+j=n+N_S} \sigma_i(\mathbf{H}_B) \sigma_j(\mathbf{H}_F) \leq \sigma_n(\mathbf{H}) \leq \min_{i+j=n+1} \sigma_i(\mathbf{H}_B) \sigma_j(\mathbf{H}_F),$$

where $(i, j) \in [N_S]^2$. The upper and lower bounds are attained respectively at

$$\begin{aligned} \Theta_{\text{sv-}n\text{-max}}^{\text{MIMO-ND}} &= \mathbf{V}_B \mathbf{P} \mathbf{U}_F^H, \\ \Theta_{\text{sv-}n\text{-min}}^{\text{MIMO-ND}} &= \mathbf{V}_B \mathbf{Q} \mathbf{U}_F^H, \end{aligned}$$

where $\mathbf{V}_B, \mathbf{U}_F \in \mathbb{U}^{N_S \times N_S}$ are any right and left singular matrices of \mathbf{H}_B and \mathbf{H}_F , respectively, and \mathbf{P} and \mathbf{Q} are arbitrary permutation matrices of dimension N_S satisfying:

- The (i, j) -th entry is 1, where

$$(i, j) = \begin{cases} \underset{i+j=n+1}{\operatorname{argmin}} \sigma_i(\mathbf{H}_B) \sigma_j(\mathbf{H}_F), & \text{for } \mathbf{P}, \\ \underset{i+j=n+N_S}{\operatorname{argmax}} \sigma_i(\mathbf{H}_B) \sigma_j(\mathbf{H}_F), & \text{for } \mathbf{Q}. \end{cases}$$

and ties may be broken arbitrarily;

- After deleting the i -th row and j -th column, the resulting submatrix \mathbf{Y} is arbitrary permutation matrix of dimension $N_S - 1$ satisfying

$$\begin{aligned} \sigma_{n-1}(\hat{\Sigma}_B \mathbf{Y} \hat{\Sigma}_F) &\geq \min_{i+j=n+1} \sigma_i(\mathbf{H}_B) \sigma_j(\mathbf{H}_F) \text{ for } \mathbf{P}, \\ \sigma_{n+1}(\hat{\Sigma}_B \mathbf{Y} \hat{\Sigma}_F) &\leq \max_{i+j=n+N_S} \sigma_i(\mathbf{H}_B) \sigma_j(\mathbf{H}_F) \text{ for } \mathbf{Q}, \end{aligned}$$

where $\hat{\Sigma}_B$ and $\hat{\Sigma}_F$ are diagonal singular value matrices of \mathbf{H}_B and \mathbf{H}_F with both i -th row and j -th column deleted, respectively.

We highlight the non-uniqueness of \mathbf{V}_B and \mathbf{U}_F . When a singular value has multiplicity k , the corresponding singular vectors can be any orthonormal basis of the k -dimensional subspace. Even if all singular values are distinct, the singular vectors of each can be scaled by a phase factor of choice.

Corollary 3.4 (Channel power gain). *If the direct channel is negligible, then the channel power gain is bounded from above (resp. below) by the inner product of squared singular values of \mathbf{H}_B*

and \mathbf{H}_F when they are sorted similarly (resp. oppositely), that is,

$$\sum_{n=1}^N \sigma_n^2(\mathbf{H}_B) \sigma_{N_S-n+1}^2(\mathbf{H}_F) \leq \|\mathbf{H}\|_F^2 \leq \sum_{n=1}^N \sigma_n^2(\mathbf{H}_B) \sigma_n^2(\mathbf{H}_F),$$

whose upper and lower bounds are attained respectively at

$$\begin{aligned} \boldsymbol{\Theta}_{\text{P-max}}^{\text{MIMO-ND}} &= \mathbf{V}_B \mathbf{U}_F^H, \\ \boldsymbol{\Theta}_{\text{P-min}}^{\text{MIMO-ND}} &= \mathbf{V}_B \mathbf{J} \mathbf{U}_F^H, \end{aligned}$$

where \mathbf{J} is the exchange (a.k.a. backward identity) matrix of dimension N_S .

As a side note, we notice [52] discussed a similar bound using extreme singular values $\max(\sigma_N(\mathbf{H}_B) \|\mathbf{H}_F\|_F^2, \sigma_N(\mathbf{H}_F) \|\mathbf{H}_B\|_F^2) \leq \|\mathbf{H}\|_F^2 \leq \min(\sigma_1(\mathbf{H}_B) \|\mathbf{H}_F\|_F^2, \sigma_1(\mathbf{H}_F) \|\mathbf{H}_B\|_F^2)$. This is a looser version of (19) and cannot take equalities unless the extreme singular values are of multiplicity N .

The upper bound (20a) is reminiscent of the optimal amplify-and-forward relay beamforming design [iii, (16), (17)] where the diagonal matrices boil down to \mathbf{I} due to the passive nature of RIS.

Corollary 3.5 (Channel capacity at general SNR). *If the direct channel is negligible, then the BD-RIS aided MIMO channel capacity is*

$$C^{\text{MIMO-ND}} = \sum_{n=1}^N \log \left(1 + \frac{s_n \sigma_n^2(\mathbf{H}_B) \sigma_n^2(\mathbf{H}_F)}{\eta} \right),$$

where η is the average noise power, $s_n = \mu - \frac{\eta}{\sigma_n^2(\mathbf{H}_B) \sigma_n^2(\mathbf{H}_F)}$ is the power allocated to the n -th mode obtainable by the water-filling algorithm [55]. The capacity-achieving BD-RIS scattering matrix is

$$\boldsymbol{\Theta}_{\text{R-max}}^{\text{MIMO-ND}} = \mathbf{V}_B \mathbf{U}_F^H.$$

Corollary 3.6 (Channel capacity at extreme SNR). *If the direct channel is negligible, then the channel capacity when the SNR ρ is very low and high are approximately bounded from above by*

$$\begin{aligned} C_{\rho_l} &\lesssim \sigma_1^2(\mathbf{H}_B) \sigma_1^2(\mathbf{H}_F), \\ C_{\rho_h} &\lesssim N \log \frac{\rho}{N} + 2 \log \prod_{n=1}^N \sigma_n(\mathbf{H}_B) \sigma_n(\mathbf{H}_F). \end{aligned}$$

1.6 The optimization problems (39) and (36) lacks of novelty. In fact, they can still be solved by the methods proposed in existing literature, e.g., [33, 57] through appropriate adjustment.

Response We agree with the reviewer that problem (36) may be solved by the method proposed in [57] with appropriate adjustment. However, extending the single mode alignment in [33] to solve problem (39) is far from optimal as shown in Fig. 8a (labelled as “Legacy”). We have added footnote 18 to clarify the novelty of our approach.

The channel power gain maximization problem is formulated as

Problem (39) has been studied in Single-Input Single-Output (SISO) [30] and Multiple-Input Single-Output (MISO) equivalents [31, 33, 40, 45] where only one mode is available. Generalizing those to MIMO is non-trivial due to trade-off between modes.

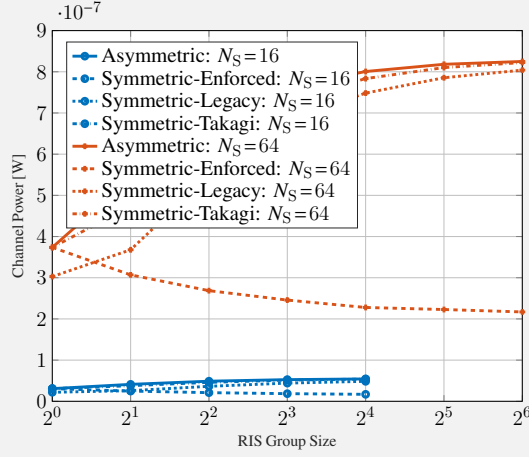


Fig. Impact of RIS symmetry on the power gain of $2 \times N_S \times 2$ MIMO point-to-point channel.

1.7 Convergence proof in Appendix J is questionable. First, the manuscript just assumes that solution iterates $\tilde{\Theta}$ converge. This may not be true (solution iterate could oscillate actually) and is hard to prove. Second, stationary point for constrained problem is more complicated than for the non-constrained case (e.g. gradient equals zero). Please refer to [iv].

Response We sincerely appreciate the reviewer for pointing out the issue. Indeed, the sequence of iterates may oscillate and the convergence proof in the previous version was incorrect. We have revised the wording in Proposition 5 and clarified the condition when a stationary point can be reached. The proof in Appendix J has been updated accordingly.

Proposition 5. Starting from any feasible $\Theta^{(0)}$, the sequence

$$\Theta_g^{(r+1)} = \mathbf{U}_g^{(r)} \mathbf{V}_g^{(r)}, \quad \forall g$$

monotonically increases the objective function (39a), where $\mathbf{U}_g^{(r)}$ and $\mathbf{V}_g^{(r)}$ are any left and right singular matrices of

$$\mathbf{M}_g^{(r)} = \mathbf{H}_{B,g}^H \left(\mathbf{H}_D + \mathbf{H}_B \text{diag}(\Theta_{[1:g-1]}^{(r+1)}, \Theta_{[g:G]}^{(r)}) \mathbf{H}_F \right) \mathbf{H}_{F,g}^H.$$

Besides, when (41) converges, (40) leads to a convergence of the objective function (39a) towards a stationary point.

However, (40) might not converge to a single solution point when \mathbf{M}_g is rank-deficient due to the non-uniqueness of the orthonormal bases of kernels.

We notice that Θ_g coincides with the orthogonal projection of \mathbf{M}_g onto the Stiefel manifold $\pi(\mathbf{M}_g) = \arg\min_{\mathbf{X}_g \in \mathbb{U}^{L \times L}} \|\mathbf{M}_g - \mathbf{X}_g\|_F = \mathbf{U}_g \mathbf{V}_g$.

Remark 1. The sequence (41) is constructed iteratively from its orthogonal projection. Although a formal proof remains elusive, empirical evidence from simulation indicates that (41) converge for vastly tested scenarios.

Reviewer 2

This paper studies the potential of a group-connected BD-RIS to manipulate the MIMO channel in terms of singular values, power gain, and achievable rate. The analysis and optimization are based on the assumption of asymmetric and lossless RIS circuit network without mutual coupling. A geodesic design framework is proposed and tested on Pareto frontier shaping and joint beamforming problems. Some analytical bounds on channel singular values and power gain are also provided. Overall, it is a solid work with interesting results. I have some further comments for the authors' reference.

2.1 *How practical is it to consider asymmetric reconfigurable BD-RIS? How much gain is expected over symmetric ones and at what cost?*

Response Asymmetric RIS may be built over asymmetric passive components (e.g., ring hybrids and branch-line hybrids). A 4-port ring hybrid is illustrated in the figure below [35].

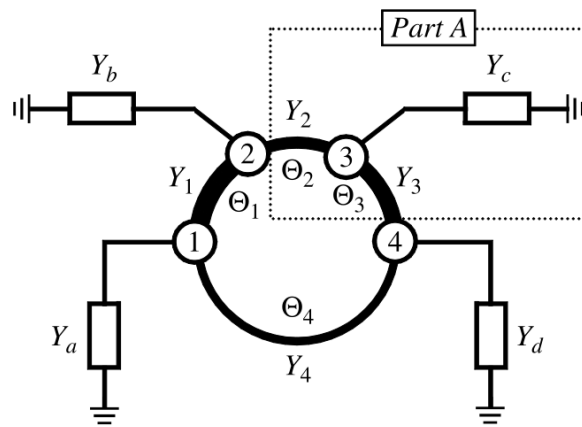


Fig. A 4-port asymmetric ring hybrid. Here the arc length between ports are $\Theta_1 = \Theta_2 = \Theta_3 = \lambda/4$ and $\Theta_4 = 3\lambda/4$ where λ is the wavelength. The termination admittances Y_a to Y_d are arbitrary and the characteristic admittances of transmission-line sections are not necessarily the same, such that the scattering parameters can be asymmetric. Source: modified from [35].

On the other hand, symmetric RIS satisfying $\Theta = \Theta^T$ are often considered in the literature as they can be implemented with simpler circuit components (e.g., capacitors and inductors). We have added Section V-D1 to investigate the impact of RIS symmetry on the system performance.

Symmetric RIS satisfying $\Theta = \Theta^T$ are often considered in the literature due to hardware constraints. This study aim to investigate the impact of RIS symmetry on the system performance.

Remark 2. All proposed asymmetric BD-RIS designs can be modified for symmetry. In particular,

- (i) *Singular Value Decomposition (SVD)-based* (e.g., (15), (20), (23), (40), (44)): Those closed-form asymmetric solutions are constructed from the product of singular matrices. If symmetry is required, one can replace the SVD of $\mathbf{A} = \mathbf{U}\mathbf{\Sigma}\mathbf{V}^H$ by the Autonne-Takagi factorization of $\frac{\mathbf{A} + \mathbf{A}^T}{2} = \mathbf{Q}\mathbf{\Sigma}\mathbf{Q}^T$ [69] and use unitary factor \mathbf{Q} to construct the corresponding Θ .
- (ii) *RCG-based* (e.g., (26), (37), (48)): The symmetry constraint is added to the corresponding optimization problems, and one can project the solution to the nearest symmetric point $\Theta \leftarrow \frac{\Theta + \Theta^T}{2}$ after each iteration.

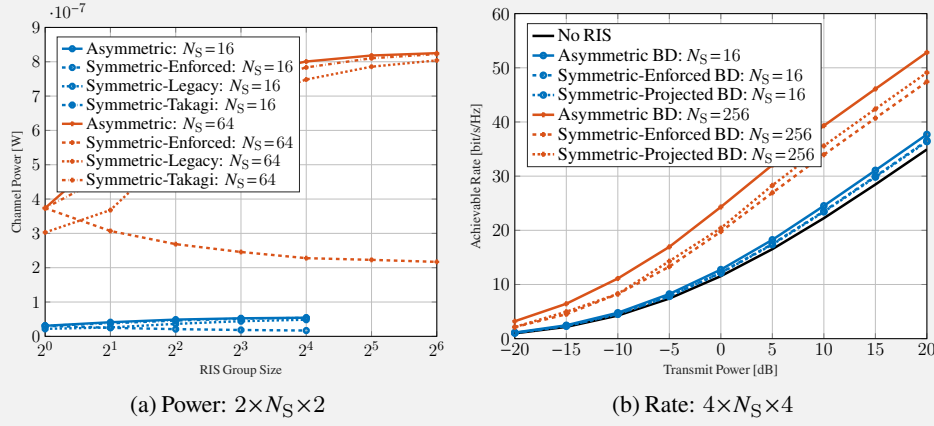


Fig. Impact of RIS symmetry on the power gain and achievable rate of MIMO point-to-point channel.

Figs. 8a and 8b compare the power gain and achievable rate of MIMO point-to-point channel under asymmetric and various symmetric RIS configurations. Here, ‘Asymmetric’ refers to the benchmark solution by (40) or (37), ‘Enforced’ refers to enforcing symmetry on ‘Asymmetric’, ‘Legacy’ refers to a straightforward extension of the SISO SNR-optimal solution [33, (6)], ‘Takagi’ refers to the modification (i), and ‘Projection’ refers to the modification (ii). We observe that the performance gaps between the asymmetric and symmetric RIS configurations are insignificant and scale with the number of scattering elements. The two proposed modifications also outperform other candidates in both problems.

2.2 *The geodesic RCG method seems promising especially at large group size L . Is it possible to extend the design framework to advanced BD-RIS architectures (e.g., multi-sector mode)?*

Response Unfortunately, the geodesic RCG method relies on the block unitary property of the BD-RIS scattering matrix and is not directly applicable to multi-sector mode BD-RIS where the constraint is relaxed to $\sum_{s=1}^S \Theta_{g,s}^H \Theta_{g,s} = \mathbf{I}, \forall g \in [G]$ with $S > 1$ sectors.

2.3 *For fully-connected BD-RIS, the authors mentioned in the result section that power gain-optimal scattering matrix is also rate-optimal. Can you provide a proof on this point?*

Response This is indeed an interesting observation. When the direct channel is negligible, the power gain-optimal scattering matrix is obtained in closed form (20a) and coincides with the rate-optimal scattering matrix (23) in the newly added Corollary 3.5. When the direct channel is significant, the observation still holds, yet unfortunately we do not have a formal proof due to the non-trivial structure of both solutions. The following context has been added to the manuscript to clarify this point.

Corollary 3.5 also suggests that the power- and rate-optimal scattering matrices (20a) and (23) coincide with each other when the direct channel is negligible and the BD-RIS is fully-connected. When either condition is not satisfied, active and passive beamforming are coupled and the rate-optimal solution involves alternating optimization. However, the power-optimal RIS still provides for a low-complexity decoupled solution. The details will be discussed in Section IV-A.

2.4 *The authors refer to [37] for estimating forward and backward channels individually. However, it can be challenging to implement those in real time without RF chains at the RIS. The impact of imperfect Channel State Information (CSI) on the achievable rates may also be studied.*

Response We agree with the reviewer that the estimation of individual forward and backward channels may be challenging in practice. Section V-D2 has been added to investigate the impact of imperfect CSI

on the proposed beamforming designs.

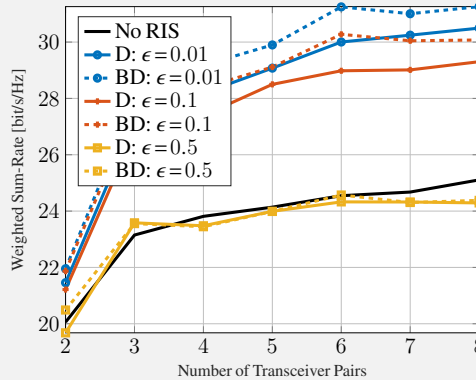


Fig. Impact of channel estimation error and transceiver pairs on the weighted sum-rate of $(2 \times 64 \times 2)^K$ MIMO interference channel with $P=20\text{dB}$ and $N_E=2$.

Fig. 9 shows the average Weighted Sum-Rate (WSR) versus the backward/forward channel estimation error and the number of transceiver pairs. Specifically, the active and passive beamformers are designed by Section IV-A1 over the estimated backward and forward channels

$$\hat{\mathbf{H}}_{\text{B/F}}^{(k)} = \mathbf{H}_{\text{B/F}}^{(k)} + \tilde{\mathbf{H}}_{\text{B/F}}^{(k)}, \quad \forall k,$$

where the error follows $\text{vec}(\tilde{\mathbf{H}}_{\text{B/F}}^{(k)}) \sim \mathcal{N}_{\mathbb{C}}(\mathbf{0}, \epsilon \Lambda_{\text{B}} \Lambda_{\text{F}} \mathbf{I})$. The WSR is evaluated using the true channels. We observe that the proposed joint beamforming design in Section IV-B1 is reasonably robust to channel estimation error and thus viable for practical implementation. On the other hand, introducing a RIS to Interference Channel (IC) systems is helpful to mitigate the rate saturation effect as K increases. In the saturated regime ($K \geq 4$), BD-RIS provides a much larger WSR than D-RIS thanks to its superior shaping capability in aligning the interference subspaces. These results provide valuable insights for practical RIS design in dense connection scenarios, where proper BD configurations can significantly enhance the network capacity.

2.5 Some sentences are confusing to me and the presentation can be improved. For example, “a group-wise geodesic RCG method that operates directly on the Stiefel manifold”. Please elaborate more on this.

Response Thank you for the feedback. The manuscript has been carefully restructured and proofread for improved clarity and readability.

Reviewer 3

This paper analyzes the channel shaping of a Point-to-Point (P2P) MIMO system, assisted by passive diagonal and/or non-diagonal RISs to enhance power and rate gains. Overall, the topic is timely and interesting. Using Alternating Optimization (AO), a local optimal solution of the rate maximization for the BD-RIS-assisted MIMO P2P system is obtained. It is shown that BD-RIS improve the achievable rate. To the best of my knowledge, the analysis is solid. However, there are some suggestions for improving the paper further.

3.1 The results for the P2P system are insightful. However, a P2P system is not typically considered a practical system. It is challenging to extend the results to a system with interfering signals, where the goal is not only to enhance the channel gain of the desired links but also simultaneously to reduce the channel gain of the interfering links. It is more interesting to investigate the rate region of K -user ICs. It is expected that the authors provide an analysis of the (max-min and sum) rate maximization of multi-user MIMO systems, assisted by BD-RISs.

Response We appreciate the reviewer's positive feedback and insightful suggestion. Interference management by RIS in multi-user MIMO systems is indeed an interesting topic. In the revised manuscript, we have extended the joint beamforming design to a K -user MIMO IC system and provided a comprehensive study on WSR maximization problem. Please refer to Sections II-C, IV-B, and V-C2 for the model, optimization, and simulation results.

We also consider a BD-RIS aided MIMO interference channel of K transceiver pairs where each transmitter and receiver has N_T and N_R antennas, respectively, and the BD-RIS has N_S scattering elements. This configuration is denoted as $(N_T \times N_S \times N_R)^K$. Let $\mathbf{H}_D^{(kj)} \in \mathbb{C}^{N_R \times N_T}$, $\mathbf{H}_B^{(k)} \in \mathbb{C}^{N_R \times N_S}$, $\mathbf{H}_F^{(j)} \in \mathbb{C}^{N_S \times N_T}$ denote the direct channel from transmitter j to receiver k , the backward channel of receiver k , and the forward channel of transmitter j , respectively, where $(j, k) \in [K]^2$. Assume all transmitter-RIS-receiver paths share the same BD-RIS scattering matrix $\mathbf{\Theta}$. The equivalent channel from transmitter j to receiver k is

$$\mathbf{H}^{(kj)} = \mathbf{H}_D^{(kj)} + \mathbf{H}_B^{(k)} \mathbf{\Theta} \mathbf{H}_F^{(j)} = \mathbf{H}_D^{(kj)} + \sum_g \mathbf{H}_{B,g}^{(k)} \mathbf{\Theta}_g \mathbf{H}_{F,g}^{(j)},$$

where $\mathbf{H}_{B,g}^{(k)} \in \mathbb{C}^{N_R \times L}$ and $\mathbf{H}_{F,g}^{(j)} \in \mathbb{C}^{L \times N_T}$ are associated with RIS group g , corresponding to the $(g-1)L+1$ to gL columns of $\mathbf{H}_{B,g}^{(k)}$ and rows of $\mathbf{H}_{F,g}^{(j)}$, respectively.

On top of (7), the achievable rate of transmission k is

$$R_k = \log \det \left(\mathbf{I} + \mathbf{W}_k \mathbf{H}^{(kj)} \mathbf{H}^{(kj)H} \mathbf{Q}_k^{-1} \mathbf{H}^{(kj)} \mathbf{W}_k \right),$$

where \mathbf{W}_k is the precoder at transmitter k and $\mathbf{Q}_k = \sum_{j \neq k} \mathbf{H}^{(kj)} \mathbf{W}_j \mathbf{W}_j^H \mathbf{H}^{(kj)H} + \eta \mathbf{I}$ is the interference-plus-noise covariance matrix at receiver k . The WSR maximization problem for BD-RIS-aided MIMO interference channel is formulated as

$$\begin{aligned} \max_{\mathbf{\Theta}, \{\mathbf{W}_k\}_{k \in [K]}} \quad & \sum_{k=1}^K \rho_k R_k \\ \text{s.t.} \quad & \mathbf{\Theta}_g^H \mathbf{\Theta}_g = \mathbf{I}, \quad \forall g, \\ & \|\mathbf{W}_k\|_F^2 \leq P_k, \quad \forall k \end{aligned}$$

where $\rho_k \geq 0$ is the weight associated with transmission k . This non-convex problem can be solved by extending both solutions covered in Section IV-A as detailed below.

On top of (7), the achievable rate of transmission k is

$$R_k = \log \det \left(\mathbf{I} + \mathbf{W}_k \mathbf{H}^{(kj)} \mathbf{H}^{(kj)H} \mathbf{Q}_k^{-1} \mathbf{H}^{(kj)} \mathbf{W}_k \right),$$

where \mathbf{W}_k is the precoder at transmitter k and $\mathbf{Q}_k = \sum_{j \neq k} \mathbf{H}^{(kj)} \mathbf{W}_j \mathbf{W}_j^H \mathbf{H}^{(kj)H} + \eta \mathbf{I}$ is the interference-plus-noise covariance matrix at receiver k . The WSR maximization problem for BD-RIS-aided MIMO interference channel is formulated as

$$\begin{aligned} \max_{\mathbf{\Theta}, \{\mathbf{W}_k\}_{k \in [K]}} \quad & \sum_{k=1}^K \rho_k R_k & (\text{ia}) \\ \text{s.t.} \quad & \mathbf{\Theta}_g^H \mathbf{\Theta}_g = \mathbf{I}, \quad \forall g, & (\text{ib}) \end{aligned}$$

$$\|\mathbf{W}_k\|_F^2 \leq P_k, \quad \forall k \quad (\text{ic})$$

where $\rho_k \geq 0$ is the weight associated with transmission k . This non-convex problem can be solved by extending both solutions covered in Section IV-A as detailed below.

Alternating Optimization

This approach updates Θ and $\{\mathbf{W}_k\}_{k \in [K]}$ iteratively until convergence. For a given precoder set, the passive beamforming subproblem is

$$\max_{\Theta} \sum_{k=1}^K \rho_k R_k \quad (\text{ia})$$

$$\text{s.t.} \quad \Theta_g^H \Theta_g = \mathbf{I}, \quad \forall g, \quad (\text{iib})$$

which can be solved optimally by Algorithm 1 with the partial derivative given in Lemma 2.

Lemma 2. *The partial derivative of (47a) with respect to BD-RIS block g is*

$$\begin{aligned} \frac{\partial \rho_k R_k}{\partial \Theta_g^*} = & \sum_{k=1}^K \rho_k \mathbf{H}_{B,g}^{(k)H} \mathbf{Q}_k^{-1} \mathbf{H}^{(kk)} \mathbf{W}_k \mathbf{E}_k \mathbf{W}_k^H \\ & \times (\mathbf{H}_{F,g}^{(k)H} - \mathbf{H}^{(kk)H} \mathbf{Q}_k^{-1} \sum_{j \neq k} \mathbf{H}^{(kj)} \mathbf{W}_j \mathbf{W}_j^H \mathbf{H}_{F,g}^{(j)H}), \end{aligned}$$

where $\mathbf{E}_k = (\mathbf{I} + \mathbf{W}_k^H \mathbf{H}^{(kk)H} \mathbf{Q}_k \mathbf{H}^{(kk)} \mathbf{W}_k)^{-1}$ is the error matrix of receiver k .

Proof. Please refer to Appendix K. \square

For a given Θ , problem (46) reduces to conventional precoding design for interference channel. A closed-form iterative solution based on mutual information-Minimum Mean-Square Error (MMSE) relationship has been proposed in [67, 68] and we summarize the steps as follows. At iteration r , the MMSE combiner at receiver k is

$$\begin{aligned} \mathbf{G}_k^{(r)} = & \mathbf{W}_k^{(r-1)H} \mathbf{H}^{(kk)H} \\ & \times (\mathbf{Q}_k^{(r-1)} + \mathbf{H}^{(kk)} \mathbf{W}_k^{(r-1)} \mathbf{W}_k^{(r-1)H} \mathbf{H}^{(kk)H})^{-1}, \end{aligned}$$

the corresponding error matrix is

$$\mathbf{E}_k^{(r)} = (\mathbf{I} + \mathbf{W}_k^{(r-1)H} \mathbf{H}^{(kk)H} \mathbf{Q}_k^{(r-1)} \mathbf{H}^{(kk)} \mathbf{W}_k^{(r-1)})^{-1},$$

and the optimal precoder at transmitter k is given by

$$\begin{aligned} \mathbf{W}_k^{(r)} = & \left(\sum_{j=1}^K \mathbf{H}^{(jk)H} \mathbf{G}_j^{(r)H} \Omega_k^{(r)} \mathbf{G}_j^{(r)} \mathbf{H}^{(jk)} + \lambda_k^{(r)} \mathbf{I} \right)^{-1} \\ & \times \mathbf{H}^{(kk)H} \mathbf{G}_j^{(r)H} \Omega_k^{(r)}, \end{aligned}$$

where $\Omega_k^{(r)} = \rho_k \mathbf{E}_k^{(r)-1}$ is the mean-square error weight and $\lambda_k^{(r)}$ is the Lagrange multiplier retrievable by bisection [67] or in closed form [68]

$$\lambda_k^{(r)} = \frac{\text{tr}(\eta \Omega_k^{(r)} \mathbf{G}_k^{(r)} \mathbf{G}_k^{(r)H} + \sum_{j=1}^K (\mathbf{Z}_{kj}^{(r)} - \mathbf{Z}_{jk}^{(r)}))}{P_k},$$

where $\mathbf{Z}_{kj}^{(r)} = \Omega_k^{(r)} \mathbf{T}_{kj}^{(r)} \mathbf{T}_{kj}^{(r)H}$ and $\mathbf{T}_{kj}^{(r)} = \mathbf{G}_k^{(r)} \mathbf{H}^{(kj)} \mathbf{W}_j^{(r)}$.

The computational complexity of solving subproblem (47) by geodesic RCG is $\mathcal{O}(I_{\text{RCG}} G(N_T d^2 + N_T^2 d + N_T^2 N_R + N_T N_R^2 + K(N_T N_R d + N_T N_R L) + I_{\text{BLS}} L^3))$. That is, $\mathcal{O}_D(N_S)$ for D-RIS and $\mathcal{O}_{\text{BD}}(N_S^3)$ for fully-connected BD-RIS.

Low-Complexity Solution

Similar to Section IV-A2, we suboptimally decouple the beamforming design by first shape the channel by RIS for minimum leakage interference and then optimize the active beamforming. The leakage interference minimization problem is formulated as

$$\begin{aligned} \min_{\Theta} \quad & I = \sum_{k=1}^K \sum_{j \neq k} \left\| \mathbf{H}_D^{(kj)} + \mathbf{H}_B^{(k)} \Theta \mathbf{H}_F^{(j)} \right\|_F^2 \\ \text{s.t.} \quad & \Theta_g^H \Theta_g = \mathbf{I}, \quad \forall g, \end{aligned}$$

which can be solved iteratively in closed form.

Proposition 6. *Starting from any feasible $\Theta^{(0)}$, the sequence*

$$\Theta_g^{(r+1)} = \mathbf{U}_g^{(r)} \mathbf{V}_g^{(r)}, \quad \forall g$$

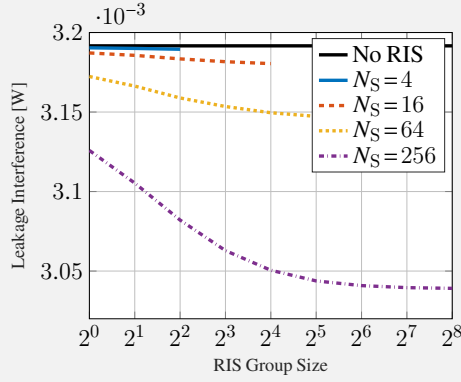
monotonically decreases the objective function (53a), where $\mathbf{U}_g^{(r)}$ and $\mathbf{V}_g^{(r)}$ are any left and right singular matrices of

$$\mathbf{M}_g^{(r)} = \sum_{k=1}^K \sum_{j \neq k} (\mathbf{B}_g^{(k)} \Theta_g^{(r)} \mathbf{H}_{F,g}^{(j)} - \mathbf{H}_{B,g}^{(k)} \mathbf{D}_g^{(kj)(r)}) \mathbf{H}_{F,g}^{(j)H},$$

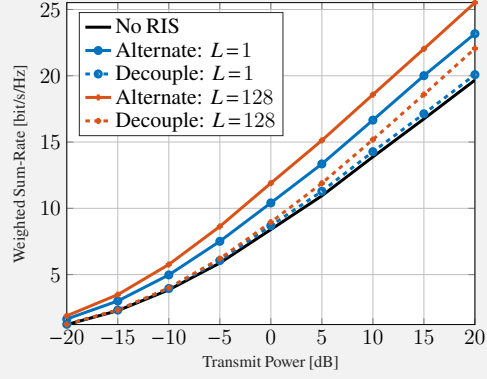
where $\mathbf{B}_g^{(k)} = \lambda_1 (\mathbf{H}_{B,g}^{(k)H} \mathbf{H}_{B,g}^{(k)}) \mathbf{I} - \mathbf{H}_{B,g}^{(k)H} \mathbf{H}_{B,g}^{(k)}$ and $\mathbf{D}_g^{(kj)(r)} = \mathbf{H}_D^{(kj)} + \sum_{g' < g} \mathbf{H}_{B,g'}^{(k)H} \Theta_{g'}^{(r+1)} \mathbf{H}_{F,g'}^{(k)} + \sum_{g' > g} \mathbf{H}_{B,g'}^{(k)H} \Theta_{g'}^{(r)} \mathbf{H}_{F,g'}^{(k)}$. Besides, when (55) converges, (54) leads to a convergence of the objective function (53a) towards a stationary point.

Proof. Please refer to Appendix L. □

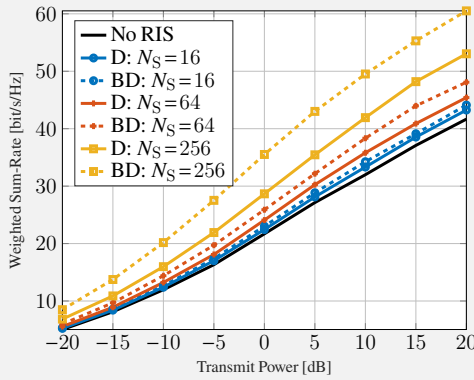
Once the channel is shaped by (54), the active beamforming is retrieved iteratively by (51). This two-stage solution avoids outer iterations and efficiently handles inner iterations.



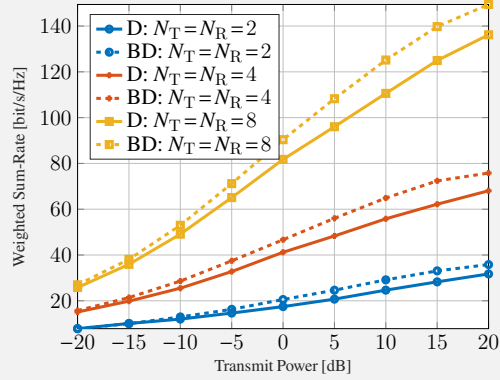
(a) Interference: $(4 \times N_S \times 4)^5$



(b) WSR: $(2 \times 128 \times 2)^2, N_E = 2$



(c) WSR: $(4 \times N_S \times 4)^5, N_E = 4$



(d) WSR: $(N_T \times 128 \times N_R)^{10}, N_E = 2$

Fig. Average leakage interference and weighted sum-rate versus RIS and MIMO interference channel configurations. ‘Alternate’ refers to the alternating optimization and ‘Decouple’ refers to the low-complexity design. ‘D’ means D-RIS and ‘BD’ refers to fully-connected BD-RIS.

Fig. 7a illustrates how BD-RIS helps to reduce the leakage interference by solving problem (53). In this case, a fully-connected 2^n -element BD-RIS is almost as good as a 2^{n+2} -element D-RIS in terms of leakage interference. The result also implies that BD-RIS can achieve a higher DoF than diagonal RIS in MIMO interference channel, which generalizes Proposition 1 and emphasizes the potential of BD-RIS in interference alignment.

Fig. 7b compares the average WSR achieved by the optimal and low-complexity beamforming designs in Section IV-B1 and IV-B2, respectively. Unlike the point-to-point case, the latter is not as effective as the former. The reason is that, for K transmissions of different path loss, interference alignment using only a shared passive beamformer is very challenging especially, when the direct channels are dominant. On the other hand, using K precoders in the joint beamforming design can reasonably orthogonalize the channels and the RIS can simply enhance the signal power. A narrower performance gap is expected when N_S increases or RIS coverage area shrinks.

Figs. 7c and 7d show the average WSR versus the number of scattering elements and transceiving antennas. Again, we observe that the rate gain of BD-RIS over D-RIS increases with N_S , N_T , and N_R . The reasons have been discussed in the point-to-point case.

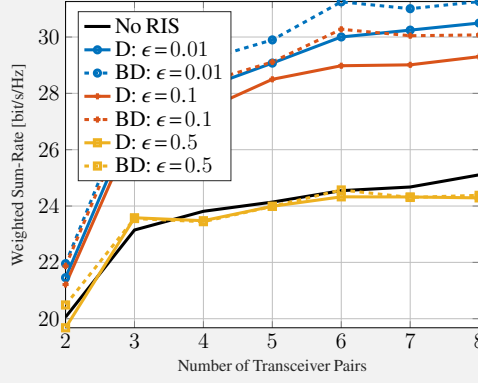


Fig. Impact of channel estimation error and transceiver pairs on the weighted sum-rate of $(2 \times 64 \times 2)^K$ MIMO interference channel with $P = 20\text{dB}$ and $N_E = 2$.

Fig. 9 shows the average WSR versus the backward/forward channel estimation error and the number of transceiver pairs. Specifically, the active and passive beamformers are designed by Section IV-A1 over the estimated backward and forward channels

$$\hat{\mathbf{H}}_{B/F}^{(k)} = \mathbf{H}_{B/F}^{(k)} + \tilde{\mathbf{H}}_{B/F}^{(k)}, \quad \forall k,$$

where the error follows $\text{vec}(\tilde{\mathbf{H}}_{B/F}^{(k)}) \sim \mathcal{N}_{\mathbb{C}}(\mathbf{0}, \epsilon \Lambda_B \Lambda_F \mathbf{I})$. The WSR is evaluated using the true channels. We observe that the proposed joint beamforming design in Section IV-B1 is reasonably robust to channel estimation error and thus viable for practical implementation. On the other hand, introducing a RIS to interference channel systems is helpful to mitigate the rate saturation effect as K increases. In the saturated regime ($K \geq 4$), BD-RIS provides a much larger WSR than D-RIS thanks to its superior shaping capability in aligning the interference subspaces. These results provide valuable insights for practical RIS design in dense connection scenarios, where proper BD configurations can significantly enhance the network capacity.

3.2 BD-RISs provide a greater number of optimization variables but at the expense of increased computational and implementation complexities. While the computational complexities of the proposed solutions are discussed in the paper, a comparison with D-RIS is missing, which should be explicitly addressed in both the introduction and the main body. Additionally, the implementation complexities of BD-RISs, particularly in comparison to D-RIS, necessitate a more comprehensive analysis. For instance, as highlighted in [v], the energy efficiency of a BD-RIS is significantly influenced by the static power consumption of its circuit elements. If the implementation cost of a BD-RIS is substantial, its performance advantages could be considerably reduced.

Response We agree with the reviewer that the computational complexities of D-RIS and fully-connected BD-RIS deserve further attention. Apart from a summary in the introduction and an explicit analysis in the main body, we have also evaluated the average statistics of the AO design for both architectures on the rate maximization problem (35).

On the other hand, the implementation complexities of BD-RIS is indeed a critical issue. An initial study has been conducted in [41] where the authors demonstrated the superior energy efficiency of BD-RIS compared to both active RIS and relay systems. Our colleagues are currently working on a more comprehensive analysis and the results will be published in a separate paper.

The additional optimization cost of BD-RIS over D-RIS is affordable and the geodesic RCG method is efficient on large-scale problems;

That is, $\mathcal{O}_D(N_S)$ for D-RIS and $\mathcal{O}_{BD}(N_S^3)$ for fully-connected BD-RIS.

Table: Performance of D-RIS and Fully-Connected BD-RIS on (35)

RIS type	$N_S = 16$			$N_S = 256$		
	Objective	Iterations (outer)	Time [s]	Objective	Iterations (outer)	Time [s]
Diagonal	25.33	2.06	2.620×10^{-2}	32.22	2.92	1.277
Fully-connected BD	26.10	3.84	2.719×10^{-2}	36.58	3.03	0.806

Table II compares the performance of D-RIS and fully-connected BD-RIS on rate maximization problem (35) using the AO design in Section IV-A1, where $N_T = N_R = 4$ and $P = 20\text{dB}$. The statistics are averaged over 100 independent runs. The fact that fully-connected BD-RIS provides a higher achievable rate using slightly more outer iterations I_{AO} than D-RIS is consistent with our analysis. Interestingly, *the former still ends up with shorter elapsed time*, which seems to contradict the complexity analysis that $\mathcal{O}_{BD}(N_S^3)$ for fully-connected BD-RIS and $\mathcal{O}_D(N_S)$ for D-RIS. One possible reason is that BD-RIS only involves 1 backtracking line search per iteration while D-RIS requires N_S times. Another reason is that the group-wise update of D-RIS leads to slower convergence of inner iterations. These results suggest that optimizing BD-RIS may be less computational intensive than expected.

3.3 *The authors considered a passive RIS architecture. However, another passive configuration, termed Globally Passive (GP), is discussed in [vi, vii]. Employing AO, the resulting optimization problem to update Θ is convex. Comparing the proposed solutions with a globally passive BD-RIS would provide valuable insights into the performance gains obtained by relaxing the (locally) passive assumption. Hence, it is highly recommended to add the GP (both BD and diagonal) architecture as a benchmark in the numerical results.*

Response We appreciate the reviewer’s suggestion and agree that the GP architecture may serve as a canonical benchmark. However, the current manuscript already exceeds the page limit and we decided not to overwhelm the readers with too many fancy RIS configurations. An in-depth comparison between GP and BD architectures holds significant value to the RIS community and deserves a separate study in the future.

References

- [i] J.-F. Cai, E. J. Candès, and Z. Shen, “A singular value thresholding algorithm for matrix completion,” *SIAM Journal on Optimization*, vol. 20, no. 4, pp. 1956–1982, 2010.
- [ii] Y. Rong and F. Gao, “Optimal beamforming for non-regenerative MIMO relays with direct link,” *IEEE Communications Letters*, vol. 13, no. 12, pp. 926–928, Dec 2009.
- [iii] Y. Rong and Y. Hua, “Optimality of diagonalization of multi-hop MIMO relays,” *IEEE Transactions on Wireless Communications*, vol. 8, no. 12, pp. 6068–6077, Dec 2009.
- [iv] J.-S. Pang, M. Razaviyayn, and A. Alvarado, “Computing B-stationary points of nonsmooth DC programs,” *Mathematics of Operations Research*, vol. 42, no. 1, pp. 95–118, Jan 2017.
- [v] M. Soleymani, I. Santamaria, E. Jorswieck, M. Di Renzo, and J. Gutiérrez, “Energy efficiency comparison of RIS architectures in MISO broadcast channels,” in *2024 IEEE 25th International Workshop on Signal Processing Advances in Wireless Communications (SPAWC)*. IEEE, Sep 2024, pp. 701–705.

- [vi] R. K. Fotock, A. Zappone, and M. D. Renzo, “Energy efficiency optimization in RIS-aided wireless networks: Active versus nearly-passive RIS with global reflection constraints,” *IEEE Transactions on Communications*, vol. 72, no. 1, pp. 257–272, 2024.
- [vii] M. Soleymani, A. Zappone, E. Jorswieck, M. D. Renzo, and I. Santamaria, “Rate region of RIS-aided URLLC broadcast channels: Diagonal versus beyond diagonal globally passive RIS,” *IEEE Wireless Communications Letters*, pp. 1–1, 2024.